Sox9 determines translational capacity during early chondrogenic differentiation of ATDC5 cells by regulating expression of ribosome biogenesis factors and ribosomal proteins

Marjolein M.J. Caron[1†*], Maxime Eveque[2†], Berta Cillero-Pastor[2], Ron M. A. Heeren[2], Bas Housmans[1], Andy Cremers[1], Mandy J. Peffers[3], Lodewijk W. van Rhijn[1], Guus van den Akker[1†], Tim J.M. Welting[1†]

[1]Laboratory for Experimental Orthopedics, Department of Orthopedic Surgery, CAPHRI Care and Public Health Research Institute, Maastricht University Medical Center. P.O. Box 5800, 6202 AZ, Maastricht, the Netherlands.
[2]Maastricht Multimodal Molecular Imaging institute (M4I), Division of Imaging Mass Spectrometry, Maastricht University Medical Center. P.O. Box 5800, 6202 AZ, Maastricht, the Netherlands.
[3]Department of Musculoskeletal Biology, Institute of Ageing and Chronic Disease, University of Liverpool, Liverpool, United Kingdom
[†] contributed equally

Running title: Sox9 influences translational capacity

Word count: 5753
Figure count: 6

*Address correspondence to:
Marjolein M.J. Caron, Ph.D.
Laboratory for Experimental Orthopedics
Department of Orthopedic Surgery
Maastricht University Medical Center
P.O. Box 5800, 6202 AZ Maastricht, the Netherlands
Phone: +31-43-3884157
e-mail: marjolein.caron@maastrichtuniversity.nl

Abstract

Introduction: In our previous research, we demonstrated that in addition to the well-known cartilage extracellular matrix-related expression of Sox9, chondrogenic differentiation of progenitor cells is driven by a sharply defined bi-phasic expression of Sox9: an immediate early and a late (extracellular matrix associated) phase expression. In this study we aimed to determine what biological processes are driven by Sox9 during the early phase of chondrogenic differentiation.

Materials: Sox9 expression in ATDC5 cells was knocked-down by siRNA transfection at the day before chondrogenic differentiation started or at day 6 in differentiation. Samples were harvested at 2 hours, and 7 days in differentiation. The transcriptomes (RNA-seq) and proteomes (LC MS/MS) were compared using pathway and network analyses. Total protein translational capacity was evaluated with the SuNSET assay, active ribosomes with polysome profiling and ribosome modus with bicistronic reporter assays.

Results: Early Sox9 knockdown severely inhibited chondrogenic differentiation weeks later. Sox9 expression during the immediate early phase of ATDC5 chondrogenic differentiation regulated the expression of ribosome biogenesis factors and ribosomal protein subunits. This was accompanied by decreased translational capacity following Sox9 knockdown, and this correlated to lower amounts of active mono- and polysomes. Moreover, cap- versus IRES-mediated translation was altered by Sox9 knockdown. Sox9 overexpression was able to induce reciprocal effects of the Sox9 knockdown.

Conclusion: Here we identified an essential new function for Sox9 during early chondrogenic differentiation. A role for Sox9 in regulation of ribosome amount, activity and composition may be crucial in preparation for the demanding proliferative phase and subsequent cartilage extracellular matrix-production of chondroprogenitors in the growth plate *in vivo*.

Keywords: ATDC5, chondrogenesis, Sox9, ribosome, translation, protein mass-spec, RNA-seq

Introduction

Chondrogenesis, or chondrogenic differentiation, is the cellular process that describes the differentiation path of progenitor cells via early mesenchymal condensation into chondrocytes that synthesize a cartilaginous extracellular matrix (ECM) (1-3). Aside from formation of articular cartilage and its maintenance, skeletal development also depends on chondrogenic differentiation. Development of the long bones of the mammalian skeleton depends on the activity of growth plates; cartilaginous entities at the ends of developing bones in which chondrocytes differentiate from progenitor cells (1-3). In contrast to articular chondrocytes, differentiating growth plate chondrocytes are predestined to undergo hypertrophic differentiation and apoptosis. The remaining cartilaginous matrix is subsequently remodelled by osteoclastic/osteocytic activity, resulting in *de novo* synthesized bone tissue (1-3). *In vivo*, chondrogenic differentiation is almost exclusively initiated from local mesenchymal progenitor cells that reside in the cartilaginous tissue (growth plate resting zone (4), articular cartilage superficial layer(5)) or in surrounding fibrous tissues (e.g. periosteum (6, 7)). *In vitro* however, chondrogenic differentiation has been reported from various primary (mesenchymal) progenitor cell sources including synovial fluid/membrane, bone marrow, adipose tissue, fibroblasts, and induced pluripotent stem cells (8-10). In addition to high amounts of oligosaccharides (hyaluronic acid, heparan sulphate, chondroitin sulfate, etc.), important cartilage ECM proteins are type II collagen (Col2a1) and aggrecan (Acan)(2, 11, 12).

The master regulator of chondrogenic differentiation is the transcription factor SRY (sex determining region Y)-box 9 (Sox9). Mutations in *SOX9* were originally identified as the cause for campomelic dysplasia (13, 14), a severe skeletal dysplasia associated with XY sex reversal and disproportionally short stature, as well as general lack of cartilaginous tissue formation. *SOX9* was found to be essential for murine early chondrogenic lineage determination (15).

Upon nuclear translocation (16, 17), Sox9 binds as a homodimer to its consensus DNA recognition sequence (A/T)(A/T)CAA(A/T)G(18), which includes the highly conserved AACAAT motif recognized by the HMG-box domain shared amongst Sox and Sry protein family members. In chondrogenic differentiation Sox9 drives the transcription of and cooperates with L-Sox5 and Sox6 for efficient transcription of the *COL2A1* and *ACAN* genes (15, 19-22). Other cartilage ECM genes have also been demonstrated to be under transcriptional control of Sox9; including *COL9A1* (23), *COL27A1* (24), and *MATN1 (25, 26).* Besides L-Sox5 and Sox6, another important factor for Sox9-mediated transcription is Smad3. Smad3 modulates the interaction between Sox9 and CBP/p300 (27), thereby possibly explaining the pro-chondrogenic effect of BMPs and TGFβs on chondrogenic differentiation (28, 29).

During chondrogenic differentiation of progenitor cells *in vitro*, induction of Sox9 expression is biphasic (30). In the first hours after initiation of chondrogenic differentiation Sox9 expression is transiently induced (immediate early Sox9 induction), together with the other members of the "Sox-trio". Sox9 expression increases a second time, in parallel with the synthesis of cartilage ECM molecules (late Sox9 induction). Previously, we showed that this immediate early Sox9 expression is in part regulated by the immediate early response gene 1 (Egr1) (31) as well as by NFκB/p65 (30). Similar expression patterns were also found in growth plate sections (30). The function of the early Sox9 induction itself remains elusive at present. In the present work we therefore determined the transcriptomic and proteomic consequences of the abrogation of early Sox9 expression during ATDC5 chondrogenic differentiation, and uncovered the biological processes that are driven by Sox9 during the early phase of chondrogenic differentiation.

Materials and methods

ATDC5 cell culture

ATDC5 cells (RIKKEN BRC, Japan, STR profiled)(32) were cultured in a humidified atmosphere at 37°C and 5% CO_2 in culture media consisting of Dulbecco's Modified Eagle Medium (DMEM)/F12 (Life Technologies, Waltham, Massachusetts, USA), 5% fetal calf serum (Life Technologies), 1% antibiotic/antimycotic (Life Technologies) and 1% non-essential amico acids (NEAA)(Life Technologies). Chondrogenic differentiation was induced by plating the cells in triplicates at 6.400 cells/cm^2, or 20.000 cells/cm^2 in transfection experiments, and addition culture media with differentiation supplements 10 μg/ml insulin (Sigma-Aldrich, St. Louis, Missouri, United States), 10 μg/ml transferrin (Roche, Basel, Switzerland), and 30 nM sodium selenite (Sigma–Aldrich). Medium was refreshed every two days.

Sox9 loss and gain of function

A small interfering RNA (siRNA) duplex for Sox9 ("Sox9 RNAi") (sense: 5'-GACUCACAUCUCUCCUAAUTT-3', anti-sense: 5'-AUUAGGAGAGAUGUGAGUCTT-3') and a scrambled siRNA duplex ("Control RNAi", Eurogentec, Seraing, Belgium) were transfected (100 nM) one day prior to initiation of chondrogenic differentiation or at day 6 in differentiation using HiPerFECT according to manufacturers' protocol (Qiagen, Hilden, Germany). A custom made DNA strand containing a start codon and 3xFLAG sequence (derived from p3xFLAG CMV7.1) and the mSox9 coding sequence (NM_011448.4:376-1899) without start codon was flanked by 5'EcoRI and 3'XbaI restriction sites (GeneCust, Boynes, France). This fragment was cloned directionally into the pLVX-EIF1α-IRES puro MCS (Takara, Saint-Germain-en-Laye, France) to generate a pLVX-EIF1α-mSox9-IRES puro

transfer plasmid. Lentiviral particles were generated according to manufacturer's instructions with the 4th generation VSV-G envelope Lenti-X system (Takara, Saint-Germain-en-Laye, France). Lentiviral titers were determined by p24 ELISA (INNOTEST HIV antigen mAb, Fujirebio, Zwijnaarde, Belgium). Viral transductions were performed by incubation of 1 ng lentivirus/cell in the presence of 8 µg/ml polybrene for 8 hours, followed by an overnight incubation with 4 µg/ml polybrene.

RNA isolation

RNA was isolated using TRIzol reagent (Life Technologies) and collecting the aqueous phase after centrifugation. RNA was precipitated with isopropanol (-80°C) and pellet by centrifugation. RNA pellets were washed in 80% ethanol and dried. RNA was dissolved in DNase/RNase-free pure water. RNA quantity and purity were determined spectrophotometrically (Biodrop, Isogen Life Sciences, Utrecht, The Netherlands).

Quantitative real time PCR

Total RNA was reverse transcribed to cDNA using standard procedures and random hexamer priming as previously described(33). Real-time quantitative PCR (RT-qPCR) was performed using Mesagreen qPCR master mix plus for SYBR Green (Eurogentec). A CFX96 Real-Time PCR Detection System (Biorad, Hercules, California, United States) was used for amplification: initial denaturation 95°C for 10 minutes, followed by 40 cycles of amplification (denaturing 15 seconds at 95°C and annealing 1 minute at 60°C). Validated primer sequences are shown in Supplemental Table 1. Data were analyzed using the standard curve method, mRNA expression was normalized to a reference gene (β-Actin) and gene expression was calculated as fold change as compared to control conditions or t=0.

RNA-sequencing and analysis

Isolated RNA was checked for quality and integrity on the Agilent 2100 Bioanalyzer (TM) via 2100 an Expert Eukaryote Total RNA Nano chip according manufacturer's protocol. The mRNA sequencing library was generated using TruSeq mRNA sample preparation kit (Illumina, Eindhoven, the Netherlands). In short, mRNA was enriched using magnetic beads coated with poly-dT, followed by fragmentation. The fragmented mRNA enriched samples were subjected to cDNA synthesis by reverse transcriptase, followed by dA-tailing and ligation of specific double-stranded bar-coded adapters. Next, the library was amplified and after cleanup the sizes of the libraries were determined on an Agilent 2100 Bioanalyzer (TM) via an DNA 1000 chip according manufacturer's protocol. Pooled libraries consisting of equal molar samples were sequenced on a high-output 75bp single read on the NextSeq500 (Illumina). For each sample, the number of treads covering one or more exons of a given transcript were extracted. Triplicates of samples that were treated with either Scrambled or Sox9 siRNAs, at two different time points, were grouped separately. A transcript was defined as expressed when all replicates of a group had at least 5 reads extracted within the transcript's region. After which the grouped data were compared to one another. The fold-change difference and the p-value were calculated using R-package edgeR (34, 35), after which the p-value was corrected for multiple testing (false discovery rate (FDR)-corrected). Transcripts having an FDR-corrected p-value <0.05, and a fold change of at least 1.5 were considered differentially expressed transcripts. EnrichR (36) software was used to display the pathways of interest obtained from the enrichment of down or up-regulated proteins. The top three pathways of interest were considered from both Wikipathways and KEGG software (version 2019, Human) based on the combined score of the p-value and the adjusted p-value scores.

Nano LC-ESI-MS/MS proteomics

At indicated time points, plates were rinsed 3 times with 1% phosphate buffered saline (PBS).

A mixture containing cOmplete Mini Protease Inhibitor Cocktail (Roche) in 25 mM ammonium bicarbonate (ABC) buffer (Sigma-Aldrich, Zwijndrecht, The Netherlands) and 6M urea (GE Healthcare, Eindhoven, The Netherlands) was added to the plates. Cells were collected by scraping with a rubber policeman and the samples were transferred to Eppendorf tubes. Triplicates were pooled and sonicated for 10 minutes and centrifuged at 12.000g for 10 min in 4°C. The final lysates were transferred to new tubes and store at -80° until further analysis. Bradford assay (Biorad, Lunteren, The Netherlands) was performed to assess protein concentration. The concentrations were adjusted to 0.2µg/µL in order to normalize for the following steps. Samples were reduced with 20mM of DTT (Sigma-Aldrich) for 45 min and alkylated with 40 mM of IAM (Sigma-Aldrich) for 45 minutes in the dark. The alkylation step was stopped by adding 20 mM of DTT. Samples were then digested by a mixture of LysC and trypsin (Promega, Leiden, The Netherlands) added at a ratio of 1:25 (enzyme:protein) and incubated for 2h at 37°C in a water bath. Finally, 200 µL of 25 mM ABC buffer was added to the samples before overnight incubation at 37°C. The digestion was stopped by adding formic acid (Sigma-Aldrich) and Acetonitrile (Biosolve) at a final concentration of 1% and 2%, respectively. 200 ng of each sample were injected for LC-MSMS analysis. The separation of the peptides was performed on a Thermo Fisher Scientific Dionex Ultimate 3000 Rapid Separation ultrahigh-performance liquid-chromatography (HPLC) system equipped with an Acclaim PepMap C18 analytical column (2µm, 75µm*150 mm, 100Å). The samples were first trapped on an online C18 column for desalting. The peptides were then separated on the analytical column with a 90-min linear gradient from 5% to 35% Acetonitrile with 0.1% formic acid (FA) at 300 nL/min flow rate. The HPLC system was coupled to a high mass resolution orbitrap MS instrument (Q-Exactive HF, Thermo Scientific, Waltham, MA). The mass spectrometer operated in data-dependent acquisition (DDA) mode with the following settings: Full MS scan of 350-1,650 *m/z* at a resolution of 120,000 at *m/z* 400, followed by tandem mass

spectrometry (MS/MS) scans for the fragmentation of the 15 most intense ions at a resolution of 30,000. The ions already selected for fragmentation were dynamically excluded for 20s. Each sample was analyzed in duplicate. For protein identification and quantification, raw files were processed within the Proteome Discoverer software (version 2.2, Thermo Scientific) using the search engine Sequest with the Swiss-Prot database *Mus musculus* (version 2017-10-25, TaxID 10090). The following parameters were used for the database search: carbamidomethylation of Cysteine for fixed modifications; oxidation of Methionine and acetylation of protein N-terminal for variable modifications; trypsin for enzyme with a maximum of two missed cleavages; y and b for the ion types with a tolerance of 10 ppm and 0.02 Da for the precursors and the fragments, respectively; minimum and maximum peptide length of 6 and 144, respectively. Normalization of the data was performed on the total peptide amount. Percolator was used for the decoy database search and the FDR was fixed at 1% maximum. A list of 21 commonly detected contaminants were removed manually. ANOVA test and principal component analysis (PCA) were performed within the Proteome Discoverer software. ANOVA test was used to analyze the statistical significance of variation observed in protein abundance between the conditions. PCA was performed on the abundance of all quantified protein to confirm and visualize the statistical significance of the protein abundance changes. The proteins were considered modulated with a p-value <0.05 and a fold change (FC) ≥ 2. EnrichR (36) software was used to display the pathways of interest obtain from the enrichment of down or up-regulated proteins. The top three pathways of interest were considered from both Wikipathways and KEGG software (version 2019, Human) based on the combined score of the p-value and the adjusted p-value scores.

Immunoblotting

Cells were lysed in RIPA buffer (150 mM NaCl, 1% NP-40, 0,5% Sodium deoxycholate, 0,1%

SDS, 50 mM Tris pH 8.0, 5.0 mM Ethylenediaminetetraacetic acid (EDTA) pH 8.0, 0.5 mM dithiothreitol (DTT) supplemented with cOmplete Mini Protease Inhibitor Cocktail (Roche) and PhosSTOP phosphatase inhibitor (Sigma-Aldrich)). Extracts were sonicated and protein concentrations were determined with a bicinchoninic acid assay (BCA) assay (Sigma-Aldrich). Proteins were separated by SDS-PAGE and transferred to nitrocellulose membranes by electroblotting. Primary antibodies for immunodetection were anti-Sox9 (Abcam, Cambridge, UK) and anti-Tubulin (Sigma-Aldrich). Bound primary anti-bodies were detected using immunoglobulins conjugated with HRP (DakoCytomation, Glostrup, Denmark) and visualized by enhanced chemoluminescence (ECL).

sGAG assay

The sulphated glycosaminoglycan (GAG) content was measured using a modified dimethyl methylene blue (DMB) assay (37). The absorbance of samples was read at 540 and 595 nm using a spectrophotometer (Multiskan FC, Life Technologies) and GAG concentrations were calculated using a chondroitin sulfate standard curve (Sigma-Aldrich) and corrected for total protein content with a BCA assay.

SUnSET assay

Protein translational capacity of ATDC5 cultures (in sextuplicates) was assessed with the SUnSET assay(38, 39). 5.4 µM puromycin (Sigma-Aldrich) was incubated for 15 minutes in the cell culture medium, immediately followed by washing in PBS and fixation for 20 minutes with 10% formalin (VWR, Radnor, Pennsylvania, United States). Permeabilization was performed for 10 minutes with 0.1% Triton X-100. Wells were rinsed with PBS with 0.1% Tween (PBS-T) and blocked for 1.5 hour with 1% (m/v) skimmed milk powder (ELK, Campina, Zaltbommel, the Netherlands) in PBS-T, followed by overnight incubation at 4°C

with the primary anti-puromycin antibody 12D10 (Sigma-Aldrich). After washing with PBS-T, wells were incubated for 1 hour at room temperature with the secondary goat anti-mouse Alexa488 antibody (Life Technologies). The fluorescent signal intensity was determined using a Tristar LB942 (Berthold, Bad Wildbad, Germany) equipped with excitation filter F485 and emission filter F353. Fluorescent data was normalized to DNA-content from the same well(40). To this end, wells were washed with HEPES-Buffered Saline (HBS), followed by 1 hour incubation with 5 µg/mL DAPI (Life Technologies) plus 5 µg/mL HOECHST 33342 (Life Technologies) in HBS. After subsequent washing steps with HBS, fluorescent signal intensity was determined using a Tristar LB942 (Berthold), using the excitation filter F355 and emission filter F460.

Polysome fractionation

Polyosome fractionation was performed basically as described previously (41). Three 15 cm plates with ATDC5 cells were used to generate a single sample. At the day of sample collection, cells were differentiated for 2 hours, then pre-treated for 5 minutes with 100 µg/ml Cycloheximide (Sigma), washed twice in 0.9% NaCl with Cycloheximide and collected by scraping with a rubber policeman in cold 0.9% NaCl. Pelleted cells were lysed for 10 minutes in 1.8 ml polysome extraction buffer (20 mM Tris-HCl (pH7.5), 100 mM KCl, 5 mM MgCl2, 0.5% Nonidet P-40, 100 µg/ml Cycloheximide, complete protease inhibitor cocktail (Roche) and RNasin (Promega, 40U/ml)) on ice. Nuclei and cellular debris were removed by centrifugation at 12.000x g for 10 minutes at 4^0C and 9/10th of the total volume was transferred to fresh tubes and measured spectrophotometrically (Nanodrop). Total yield was the same for siCtrl and siSox9 treated cells. Sucrose gradients (linear 10-50%) were made with the Gradient Master (BioComp) in ultracentrifuge tubes (Seton, SW41 tubes). Cytoplasmic extracts (250 µg/sample) were loaded to each gradient in a fixed volume (400 µl). Gradients were run on an

ultra-centrifuge (Beckman L60) at 39.000 rpm for 1.5 hours at 4^0C with max acceleration and deceleration 9. Samples were fractionated into 24 x 0.5 ml fractions using a Piston Gradient fractionator (BioComp) and fraction collector (Gilson FC203B) with continuous A260 monitoring (Triax FC-1).

Bicistronic reporter assay

Reporter constructs for the CrPv IGR IRES, the CrPv CCGG IGR IRES mutant, the HCV and the P53 IRES were a kind gift of Dr. S. Thompson. One day post plating, maxi-prep DNA (0.5 µg/well) and 100 nM siRNA were transfected into 24-wells wells (n=3/group) using Mirus Transit-X2 according to manufacturer's instructions. The next day differentiation was induced for 24 hours, samples were collected by washing cells with 0.9% NaCl and incubation in 100 µl passive lysis buffer for 15 minutes (Promega). Subsequently, samples were transferred to Eppendorf tubes and centrifuged for 10 minutes at 12.000x g in a tabletop centrifuge. Next, 50 µl lysate was used for dual luciferase measurements (Promega) using a Berthold injection system (10 seconds counting time per cistron). Data is represented as fold change of the ratio Fluc/Rluc in control cells for each IRES.

Statistics in other than proteomics or transcriptomic analysis

Statistical significance was determined by two-tailed student t-tests using Graphpad PRISM 5.0 (La Jolla, CA, USA). Due to small sample size (n=3 samples) normal distribution of input data was assumed. Error bars in graphs represent mean ± standard error of the mean. Significance for all tests was set at $p \leq 0.05$.

Results

Early Sox9 peak in ATDC5 chondrogenic differentiation

During chondrogenic differentiation of progenitor cells in vitro, induction of Sox9 expression is bi-phasic (30, 31). In the first (2-4) hours after initiation of chondrogenic differentiation of ATDC5 cells Sox9 expression was transiently induced on mRNA (Figure 1A) and protein level (Figure 1B). Sox9 expression increased a second time in differentiation around day 7 in differentiation (Figure 1A), in parallel with the expression of the important Sox9 transcriptional target Col2a1 (21) (Figure 1C) and gain of glycosaminoglycan (GAG) content (2, 19) (Figure 1D). The immediate early transient Sox9 expression peak at 2 hours in differentiation did not correlate with the induction of expression of well-known Sox9 transcriptional targets such as Col2a1. Hence, we questioned what the function of the early Sox9 expression peak (2 hours) is and how it differs from the later Sox9 activity (day 7). We approached this question by performing a loss-of-function experiment and comparing the Sox9-dependent transciptome and proteome in an unbiased manner.

Transcriptome and proteome analysis at 2 hours and 7 days in ATDC5 chondrogenic differentiation under Sox9 knockdown

To target early Sox9 expression, a siRNA for Sox9 or scrambled control siRNA were transfected one day prior to initiation of differentiation (t = -1d) (Figure 2A). At t=0 chondrogenic differentiation was induced and cells were differentiated for 14 days. We established effective knockdown of Sox9 at t=0 and t=2 hours in differentiation, while at day 5, 7 and 14 in differentiation Sox9 mRNA levels returned to scrambled siRNA control conditions (Figure 2B; black bars and Figure 2C). In parallel, ATDC5 cells were differentiated and the siRNA for Sox9 or scrambled siRNA were transfected at day 6 in differentiation, to

specifically target expression of “late” Sox9 induction. Effective knockdown of Sox9 at day 7 and day 14 was observed at mRNA as well as (Figure 2B; grey bars) on protein level (Figure 2C). To understand the function of the immediate early Sox9 expression at 2 hours in differentiation as compared to the late Sox9 induction present at day 7 in differentiation, we subsequently used an unbiased transcriptomics and proteomics approach. Differential expression of mRNAs and proteins was determined between the control scrambled siRNA condition versus Sox9 siRNA knockdown condition at 2 hours as well as at 7 days in ATDC5 differentiation (Figure 2D).

The extracted RNA was used for RNA sequencing and Principal Component Analysis (PCA) confirmed that samples from the control scrambled siRNA condition at 2 hours and at 7 days were separated from Sox9 siRNA knockdown samples at 2 hours and 7 days (Supplementary Figure 1A). Noteworthy, the separation between the scrambled siRNA and Sox9 siRNA conditions was particularly evident at 2 hours, while separation between the scrambled siRNA and Sox9 siRNA conditions at 7 days was less obvious. At 2 hours in ATDC5 chondrogenic differentiation, knockdown of Sox9 led to the differential expression of 2422 genes, with 1235 upregulated genes and 1187 downregulated genes (Figure 2E/F). At 7 days in differentiation 493 genes were differentially expressed due to knockdown of Sox9. From these differentially expressed genes, 203 genes were upregulated (only 15 overlapped with the 2 hour time point) and 290 genes were downregulated (49 genes overlapped with the 2 hours condition) (Figure 2E/F). All genes that were differentially expressed ($FC \geq 2$; $p < 0.05$) at 2 hours and at 7 days in ATDC5 chondrogenic differentiation following Sox9 knockdown, are shown in Supplementary Tables 2 and 3, respectively.

Extracted protein samples from control conditions and Sox9 knockdown conditions at 2 hours and 7 days in ATDC5 differentiation were used for LC MS/MS with label free quantification. PCA plotting confirmed that control samples at 2 hours clearly separated from the Sox9

knockdown samples at 2 hours in ATDC5 differentiation. Separation between control and Sox9 knockdown conditions was also confirmed at 7 days in chondrogenic differentiation. However, and in concert with the PCA plot of the RNA sequencing data (Supplementary Figure 1A), the separation between control and Sox9 knockdown conditions appeared to be most obvious at 2 hours in differentiation (Supplementary Figure 2A). At 2 hours in differentiation, knockdown of Sox9 caused the differential expression of 90 proteins, with the expression of 29 proteins being upregulated and 61 proteins downregulated (Figure 2G/H and Supplemental Figure 2B). At 7 days in differentiation, the knockdown of Sox9 induced differential expression of 19 proteins. Of these 19 proteins, the expression of 9 proteins was upregulated and 10 proteins were downregulated. There was no overlap between the Sox9-dependent differentially expressed proteins at 2 hours or at 7 days in differentiation (Figure 2G/H and Supplemental Figure 2B). The proteins that were differentially expressed ($FC \geq 2$; $p < 0.05$) at 2 hours and at 7 days in ATDC5 chondrogenic differentiation following gSox9 knockdown, are shown in Supplementary Tables 4 and 5, respectively.

These data indicate that at 2 hours in chondrogenic differentiation the knockdown of Sox9 induced different changes in the ATDC5 transcriptome and proteome when compared to knockdown of Sox9 at 7 days in differentiation. In addition, the consequences of Sox9 siRNA treatment appears to be stronger at 2 hours than at 7 days of differentiation, as indicated by larger separation in the PCA plots and larger number of differentially expressed genes and proteins. The role of the immediate early Sox9 expression was further investigated by comparing the Sox9-dependent differentially expressed mRNAs and proteins at 2 hours in differentiation, since differences in mRNA expression are expected to reflect on differences in protein expression. Figure 2I and 2J show 4 overlapping mRNAs and proteins upregulated in the early Sox9 knockdown condition (Rps30/Fau, Avan, Eefsec, Rpl38; Supplementary Table 6) and 3 overlapping mRNAs and proteins downregulated in the early Sox9 knockdown

condition (Ube2d3, Dclk1, Svil; Supplementary Table 6). Except for Rpl38, these overlapping targets are unique for the 2 hour in differentiation time point.

Immediate early Sox9 expression is involved in ribosomal protein expression

To determine which prominent pathways link to the Sox9-dependent differential transcriptome and proteome at 2 hours in differentiation, we performed pathway analyses. Both WikiPathways and KEGG Pathway analyses revealed that "Cytoplasmic Ribosomal Proteins" and "Ribosome" pathways were in the top three of identified enriched pathways (Figure 3). This strong overrepresentation of the "Cytoplasmic Ribosomal Proteins" and "Ribosome" pathways was not obvious in the Sox9-dependent differential transcriptome and proteome at day 7 in differentiation (Supplementary Table 7). Further analysis of the 2 hours Sox9-dependent transcriptome datasets revealed the differential expression of 29 ribosomal protein encoding genes from the large (60S) ribosomal subunit (Rpls) and 10 ribosomal proteins from the small (40S) ribosomal subunit (Rpss) in the Sox9 knockdown condition at 2 hours in ATDC5 chondrogenic differentiation (Figure 4A and Supplementary Table 2). In addition, the 2 hours proteomics datasets demonstrated the differential expression of 5 ribosomal Rpl and Rps proteins (Figure 4A and Supplementary Table 4). Notably, the 4 overlapping mRNAs and proteins (Rps30/Fau, Avan, Eefsec, Rpl38) that were found to be upregulated in the Sox9 knockdown condition at 2 hours in ATDC5 chondrogenic differentiation (Figure 2I and Figure 4B) are all linked to protein translation and represent either ribosomal protein subunits or factors with a known function in ribosome biogenesis. Additional factors involved in ribosome biogenesis, but only differentially expressed in either the 2 hours transcriptomics or proteomics datasets were SBDS, Nop10 and Brix1 (Supplementary Tables 2 and 3 and Figure 4B). Since ribosomes do not only consist of proteins, but depend on structural and catalytically active ribosomal RNAs (rRNAs), we investigated whether rRNA levels were affected by the Sox9

knockdown at 2 hours in differentiation in ATDC5. Expression of 18S rRNA, 28S rRNA and 5.8S rRNA was not significantly different between the conditions (Figure 4C). Together, these data indicate that the immediate early Sox9 expression during ATDC5 chondrogenic differentiation is involved in expression of ribosomal proteins and proteins involved in ribosome biogenesis.

Early Sox9 expression regulates protein translation capacity and ribosome translation modus

Since we identified the differential expression of ribosomal protein subunits and ribosome biogenesis factors, combined with unaltered rRNA expression levels, we hypothesized that ribosomes of early Sox9 knockdown ATDC5 cells are functionally distinct. To address this hypothesis, we measured total translational capacity, performed polysome fractionation and evaluated ribosome translation modus in Sox9 knockdown and control ATDC5 cells. Following the knockdown of immediate early Sox9 expression a reduction of the total protein translational capacity was observed at 2 hours in chondrogenic differentiation (Figure 5A). The abrogation of early Sox9 expression also caused a reduction of total protein translational capacity measurable at day 7 in differentiation (while Sox9 levels normalized at 7 days following the early knockdown (Figure 2B)). This impact on translation capacity was lost at day 14 in differentiation (Figure 5A). In contrast, late knockdown of Sox9 expression did not affect ATDC5 translational capacity at 7 days in chondrogenic differentiation. This is consistent with transcriptome and proteome data. To assess if Sox9 knock-down had a specific effect on active monosomal or polysomal ribosomes, we performed sucrose density gradient separation of ribosomal subunits (40S and 60S), 80S monosomes and polysomes. With equal loading of cytoplasmic extracts, knockdown of the immediate early Sox9 expression resulted in an overall lower abundance of ribosomal subunits, monosomes and polysomes at 2 hours in ATDC5 chondrogenic differentiation (Figure 5B). In addition to total ribosome translation capacity

(Figure 5A), the modus of translation is also subject to regulation. Thus, we evaluated the activity of IRES (internal ribosome entry site)- over cap-mediated protein translational activity using well-known IRES bicistronic reporter constructs (CrPv IGR, HCV and P53) (42-44). We observed a 1.5-fold induction of the ITAF (IRES trans-acting factor) independent CrPv IGR IRES activity and 5-fold down regulation of both the HCV and P53 IRES activity in Sox9 knockdown ATDC5 cells compared to controls (Figure 5C, and Supplementary Figure 3). We next investigated whether overexpression of Sox9 levels during early ATDC5 differentiation may have a reciprocal effect on the translation capacity as opposed to the Sox9 knockdown conditions. Overexpression of Sox9 was confirmed (Figure 6A) and the mRNA expression of the Sox9 transcriptional target Col2a1 was significantly induced by Sox9 overexpression (Figure 6A). The overexpression of Sox9 resulted in a significant increase in translational capacity at 2 hours in ATDC5 differentiation (Figure 6B). This increase in translational capacity in the Sox9 overexpression condition was not accompanied by an increase in expression of rRNAs (Figure 6C). Reciprocally to the knockdown of Sox9 (Figure 4B), expression of ribosomal protein subunits Rpl38 and Rps30/Fau was significantly downregulated when Sox9 was overexpressed (Figure 6D). This was also the case for ribosome biogenesis factors Nop10 and SBDS (Figure 6D).

Taken together, knockdown of early Sox9 expression during ATDC5 chondrogenic differentiation reduced protein translational activity over a seven-day time period, which was reflected by a general reduction of A_{260} signal in a polysome fractionation experiment at 2 hours in differentiation. This was associated with a differential effect on ribosome translation modus during the first day of differentiation. Sox9 overexpression during early ATDC5 differentiation was able to induce reciprocal effects of the Sox9 knockdown.

Discussion

Early chondrogenic lineage commitment during mesenchymal condensation is driven by Sox9 (15, 45, 46). Following lineage commitment, Sox9 is a key regulator of cartilage extracellular matrix (ECM) synthesis, by driving expression of key ECM molecules like Acan, Col2a1 and others (15, 19-26). Sox9 also safeguards maintenance of articular cartilage homeostasis by influencing chondrocyte Nkx3-2 levels, a transcriptional repressor of chondrocyte hypertrophy (47, 48). This dual action of Sox9 is recapitulated in in vitro models of chondrogenic differentiation, as we have previously reported on bi-phasic expression dynamics of Sox9 in ATDC5 and BMSC chondrogenic differentiation (30, 31). In this earlier work we demonstrated that early (hours) transient induction of Sox9 expression driven by NFκB/p65 or Egr1 in ATDC5 chondrogenic differentiation is a prerequisite for late-stage (days) expression of cartilage ECM genes. As a key transcription factor for cartilage, the vast majority of investigations on the downstream functions of Sox9 have mainly focussed on its role in the transcriptional regulation of cartilage ECM genes (15, 19-26). In addition, a function in epigenetic reprogramming has been suggested for early Sox9 (31) , as well as a role for Sox9 in activating super-enhancers in chondrocytic cells (49). However, its downstream cell biological consequences during early chondrogenic differentiation are incompletely understood. The present study demonstrates that Sox9 expression during the very early phase of ATDC5 chondrogenic differentiation regulates the expression of ribosomal protein subunits, as well as proteins that are involved in ribosome biogenesis, that together modulate ribosome activity and translation modus. These data, for the first time, connect the Sox9 transcription factor to regulation of protein translation during chondrogenic differentiation.

Ribosomopathies are severe genetic diseases caused by mutations in genes involved in ribosome biogenesis and -function and are, amongst others, associated with developmentally-

related skeletal malformations, caused by impairment of chondrogenic development of the growth plates (50, 51). This indicates that chondrogenic differentiation is particularly susceptible for disturbances in ribosome protein translation activity. Indeed, during chondrogenesis, a large amount of proteinaceous cartilage ECM is produced by the developing growth plate and disturbances in ribosome activity are likely to impair ECM synthesis, with consequences for the development of skeletal elements. It should however be noted that the link between Sox9 and chondrocyte translation activity in the present work was particularly present during early differentiation rather than late differentiation. This is highlighted by deregulated expression of ribosomal subunits following Sox9 knockdown in early ATDC5 chondrogenic differentiation (Figure 3 and 4). In addition, the knockdown of Sox9 specifically impacted total protein translation throughout differentiation when knocked-down early, while not having an effect on protein translation when knocked-down during late chondrogenic differentiation (Figure 5). The link between early Sox9 and chondrocyte protein translation suggests that protein translation is likely to be paced through Sox9 during early chondrogenic differentiation However, it remains to be determined how early Sox9 is specifically able to influence chondrocyte translational capacity. Our present data suggest that expression of ribosomal protein subunits, ribosome biogenesis factors and ancillary ribosomal factors (such as IRES trans-acting factors (ITAFs)) depends on Sox9 during early chondrogenic differentiation, with downstream consequences for translation in the later differentiation program. Since we found these ribosomal genes and proteins differentially expressed after Sox9 knockdown, we studied the supplementary data of previously published Sox9 ChIP-seq and $Sox9^{-/-}$ mouse studies (46, 49). In supplementary data of a Sox9 ChIP-seq study we found 24 Rps and Rpl genes that were enriched in Sox9 occupancy and 14 with Sox6 occupancy of which 10 overlapped (49). Notably, this included Rpl38, which we found to be differentially expressed at the mRNA and protein level in our present Sox9 knockdown condition.

Aside from ribosome core components, we identified Sox9-dependent differential expression of several factors regulating the mode of protein translation. The rate-limiting step of cap-mediated translation is eukaryotic initiation factor 4. Interestingly, EIF4BP2 was downregulated at the protein level at 2 hours of differentiation in Sox9 knockdown cells. EIF4 binding proteins were shown to regulate cell proliferation, but not cell size (52). Unexpectedly, we found strong differences in IRES activity upon early Sox9 knockdown after 24 hours of differentiation. Of note, the CrPv IGR IRES (a type IV IRES (REF)) does not require ITAFs and is able to recruit the ribosome directly for translation (53). The activity of this IRES was increased and might be regulated by specific Rps/Rpls that transiently interact with the core ribosome components. The HCV (a type III IRES) and P53 IRES do require additional ITAF co-factors (54). Based on the increased expression of the ITAF Rpl38, it is tempting to speculate that other ITAFs that facilitate HCV/P53 IRES translation are down regulated and may contribute to alternative use of ribosome translation modus. Rpl10a, Rpl11, Rpl38 and Pdcd4 were shown to regulate IRES-mediated translation (54). Rpl10a is known to activate the *IGF2, APP, Chmp2A* and *Bcl-2* IRESs. Gain- and loss-of-function studies in *Drosophila* showed that *Rpl10a* regulates insulin signaling (55). Moreover, *Rpl10a* mRNA was found to be preferentially translated by a subpool of ribosomes in embryonic stem cells that required ribosome-associated *Rpl10a* protein (56). Insulin and IGF1 signaling are crucial for ATDC5 differentiation (32). Rpl11 induced the *BAG1, CSDE1* and *LamB1* IRESs, while *Rpl38* activated a Hox gene IRES. Upregulation of *Rpl11* led to stabilization of P53 and reduced proliferation of breast cancer cell-lines (57). In contrast, we found a reduction in *P53* IRES activity. Of note, P53 and ribosome biogenesis were recently coupled through SBDS (58). In our dataset, SBDS was down regulated at the protein level at 2 hours in differentiation in Sox9 siRNA treated cells, which matches with the observed reduction in ribosomes and/or ribosome activity. Pdcd4 activated or inhibited the P53, INR, IGF1R, BcL-XL and XIAP IRESs (54). The IGF1R IRES

might again be relevant for the ATDC5 differentiation model. Finally, Rpl38 was the only ITAF that was found to be upregulated at both the mRNA and protein level. It was found to control HOX gene translation during murine embryonic development (59) and knockout led to ectopic mineralization in certain soft tissues (60).

Together we identified multiple connections between immediate early Sox9 expression during ATDC5 chondrogenic differentiation and downstream consequences for expression of ribosomal protein subunits, ribosome biogenesis factors and ITAFs. The connection between Sox9 expression and protein translation appears to be centered in early chondrogenic differentiation, with consequences for protein translation in later stage of chondrogenic differentiation. This suggests a role for early Sox9 in the priming of progenitor cells in the chondrogenic differentiation program for cartilaginous ECM production later in differentiation. This provides a new level of understanding how Sox9 controls the fate of chondrogenic differentiation at the level of protein synthesis. In this respect it is tempting to speculate on the classification of campomelic dysplasia (OMIM #114290) (61), as links between Sox9 and genes involved in ribosomopathies (50, 62) were identified in the present work (SBDS, Rpl11, Rps26). In conclusion, we here collected essential new data on the regulation by Sox9 during early chondrogenic differentiation, uncovering an unanticipated role of Sox9 in ribosome biogenesis and protein translational capacity.

Acknowledgements

This work was financially supported by the Dutch Arthritis Association (grant LLP14) and by the Dutch Province of Limburg through the "LINK" program and by the MUMC institutional grant for clinical collaborative research. The funders had no role in study design, data collection, and analysis, decision to publish, or preparation of the manuscript.

Contribution to the Field Statement

In our previous research, we demonstrated that chondrogenic differentiation of progenitor cells is driven by a sharply defined bi-phasic expression of Sox9: an immediate early and a late phase expression. The late phase expression of Sox9 is associated with cartilage extracellular matrix formation, while the function of the early Sox9 induction itself remains elusive at present. In this study we aimed to determine what biological processes are driven by Sox9 during the early phase of chondrogenic differentiation. We identified an essential new function for Sox9 during early chondrogenic differentiation. A role for Sox9 in regulation of ribosome amount, activity and composition was found and may be crucial in preparation for the demanding proliferative phase and subsequent cartilage extracellular matrix-production of chondroprogenitors in the growth plate in vivo.

Conflict of interest

MMJ Caron and TJM Welting are inventor on patents WO2017178251 and WO2017178253 (licensed to Chondropeptix). LW van Rhijn and TJM Welting have shares in Chondropeptix and are CDO and CSO of Chondropeptix. All other authors have no competing interests to declare.

Funding

This work was financially supported by the Dutch Arthritis Association (grant LLP14) and by the Dutch Province of Limburg through the “LINK” program and by the MUMC institutional grant for clinical collaborative research. The funders had no role in study design, data collection, and analysis, decision to publish, or preparation of the manuscript.

Data Availability Statement

The datasets used and/or analyzed during the current study are available from the corresponding author on reasonable request. RNAseq transcriptomics and Nano LC-ESI-MS/MS proteomics are deposited in xxx

Email addresses of all authors:
marjolein.caron@maastrichtuniversity.nl
m.eveque@maastrichtuniversity.nl
b.housmans@maastrichtuniversity.nl
a.cremers@maastrichtuniversity.nl
b.cilleropastor@maastrichtuniversity.nl
r.heeren@maastrichtuniversity.nl
m.j.peffers@liverpool.ac.uk
l.van.rhijn@mumc.nl
g.vandenakker@maastrichtuniversity.nl
t.welting@maastrichtuniversity.nl

References

1. H. M. Kronenberg: Developmental regulation of the growth plate. *Nature*, 423(6937), 332-6 (2003)
2. V. Lefebvre and P. Smits: Transcriptional control of chondrocyte fate and differentiation. *Birth Defects Res C Embryo Today*, 75(3), 200-12 (2005) doi:10.1002/bdrc.20048
3. E. J. Mackie, Y. A. Ahmed, L. Tatarczuch, K. S. Chen and M. Mirams: Endochondral ossification: how cartilage is converted into bone in the developing skeleton. *Int J Biochem Cell Biol*, 40(1), 46-62 (2008)
4. V. Abad, J. L. Meyers, M. Weise, R. I. Gafni, K. M. Barnes, O. Nilsson, J. D. Bacher and J. Baron: The role of the resting zone in growth plate chondrogenesis. *Endocrinology*, 143(5), 1851-7 (2002) doi:10.1210/endo.143.5.8776
5. C. Karlsson and A. Lindahl: Articular cartilage stem cell signalling. *Arthritis research & therapy*, 11(4), 121 (2009) doi:10.1186/ar2753
6. H. Nakahara, S. P. Bruder, V. M. Goldberg and A. I. Caplan: In vivo osteochondrogenic potential of cultured cells derived from the periosteum. *Clin Orthop Relat Res*(259), 223-32 (1990)
7. P. J. Emans, M. M. J. Caron, L. W. van Rhijn, V. P. Shastri and T. J. M. Welting: Cartilage Tissue Engineering; Lessons Learned From Periosteum. *Tissue Science & Engineering*, S2:002 (2011) doi:doi:10.4172/2157-7552.S2-002
8. F. P. Barry and J. M. Murphy: Mesenchymal stem cells: clinical applications and biological characterization. *The international journal of biochemistry & cell biology*, 36(4), 568-84 (2004) doi:10.1016/j.biocel.2003.11.001
9. M. M. French, S. Rose, J. Canseco and K. A. Athanasiou: Chondrogenic differentiation of adult dermal fibroblasts. *Ann Biomed Eng*, 32(1), 50-6 (2004) doi:10.1023/b:abme.0000007790.65773.e0
10. S. P. Medvedev, E. V. Grigor'eva, A. I. Shevchenko, A. A. Malakhova, E. V. Dementyeva, A. A. Shilov, E. A. Pokushalov, A. M. Zaidman, M. A. Aleksandrova, E. Y. Plotnikov, G. T. Sukhikh and S. M. Zakian: Human induced pluripotent stem cells derived from fetal neural stem cells successfully undergo directed differentiation into cartilage. *Stem cells and development*, 20(6), 1099-112 (2011) doi:10.1089/scd.2010.0249
11. B. de Crombrugghe, V. Lefebvre and K. Nakashima: Regulatory mechanisms in the pathways of cartilage and bone formation. *Curr Opin Cell Biol*, 13(6), 721-7 (2001)
12. H. Mankin, V. Mow and J. Buckwalter: Articular cartilage structure, composition, and function. AAOS, Rosemont (2000)
13. J. W. Foster, M. A. Dominguez-Steglich, S. Guioli, C. Kwok, P. A. Weller, M. Stevanovic, J. Weissenbach, S. Mansour, I. D. Young, P. N. Goodfellow and et al.: Campomelic dysplasia and autosomal sex reversal caused by mutations in an SRY-related gene. *Nature*, 372(6506), 525-30 (1994) doi:10.1038/372525a0
14. T. Wagner, J. Wirth, J. Meyer, B. Zabel, M. Held, J. Zimmer, J. Pasantes, F. D. Bricarelli, J. Keutel, E. Hustert, U. Wolf, N. Tommerup, W. Schempp and G. Scherer: Autosomal sex reversal and campomelic dysplasia are caused by mutations in and around the SRY-related gene SOX9. *Cell*, 79(6), 1111-20 (1994)
15. H. Akiyama, M. C. Chaboissier, J. F. Martin, A. Schedl and B. de Crombrugghe: The transcription factor Sox9 has essential roles in successive steps of the chondrocyte differentiation pathway and is required for expression of Sox5 and Sox6. *Genes Dev*, 16(21), 2813-28 (2002) doi:10.1101/gad.1017802
16. A. Argentaro, H. Sim, S. Kelly, S. Preiss, A. Clayton, D. A. Jans and V. R. Harley: A SOX9 defect of calmodulin-dependent nuclear import in campomelic dysplasia/autosomal sex reversal. *The Journal of biological chemistry*, 278(36), 33839-47 (2003) doi:10.1074/jbc.M302078200
17. D. R. Haudenschild, J. Chen, N. Pang, M. K. Lotz and D. D. D'Lima: Rho kinase-dependent activation of SOX9 in chondrocytes. *Arthritis and rheumatism*, 62(1), 191-200 (2010) doi:10.1002/art.25051
18. S. Mertin, S. G. McDowall and V. R. Harley: The DNA-binding specificity of SOX9 and other SOX proteins. *Nucleic acids research*, 27(5), 1359-64 (1999)
19. Y. Han and V. Lefebvre: L-Sox5 and Sox6 drive expression of the aggrecan gene in cartilage by securing binding of Sox9 to a far-upstream enhancer. *Mol Cell Biol*, 28(16), 4999-5013 (2008) doi:10.1128/MCB.00695-08
20. V. Lefebvre, R. R. Behringer and B. de Crombrugghe: L-Sox5, Sox6 and Sox9 control essential steps of the chondrocyte differentiation pathway. *Osteoarthritis Cartilage*, 9 Suppl A, S69-75 (2001)
21. V. Lefebvre, W. Huang, V. R. Harley, P. N. Goodfellow and B. de Crombrugghe: SOX9 is a potent activator of the chondrocyte-specific enhancer of the pro alpha1(II) collagen gene. *Mol Cell Biol*, 17(4), 2336-46 (1997)
22. V. Lefebvre, P. Li and B. de Crombrugghe: A new long form of Sox5 (L-Sox5), Sox6 and Sox9 are coexpressed in chondrogenesis and cooperatively activate the type II collagen gene. *EMBO J*, 17(19), 5718-33 (1998) doi:10.1093/emboj/17.19.5718
23. M. A. Genzer and L. C. Bridgewater: A Col9a1 enhancer element activated by two interdependent SOX9 dimers. *Nucleic acids research*, 35(4), 1178-86 (2007) doi:10.1093/nar/gkm014
24. E. Jenkins, J. B. Moss, J. M. Pace and L. C. Bridgewater: The new collagen gene COL27A1 contains

SOX9-responsive enhancer elements. *Matrix biology : journal of the International Society for Matrix Biology*, 24(3), 177-84 (2005) doi:10.1016/j.matbio.2005.02.004
25. C. D. Oh, S. N. Maity, J. F. Lu, J. Zhang, S. Liang, F. Coustry, B. de Crombrugghe and H. Yasuda: Identification of SOX9 interaction sites in the genome of chondrocytes. *PLoS One*, 5(4), e10113 (2010) doi:10.1371/journal.pone.0010113
26. O. Rentsendorj, A. Nagy, I. Sinko, A. Daraba, E. Barta and I. Kiss: Highly conserved proximal promoter element harbouring paired Sox9-binding sites contributes to the tissue- and developmental stage-specific activity of the matrilin-1 gene. *The Biochemical journal*, 389(Pt 3), 705-16 (2005) doi:10.1042/BJ20050214
27. T. Furumatsu, M. Tsuda, N. Taniguchi, Y. Tajima and H. Asahara: Smad3 induces chondrogenesis through the activation of SOX9 via CREB-binding protein/p300 recruitment. *The Journal of biological chemistry*, 280(9), 8343-50 (2005) doi:10.1074/jbc.M413913200
28. W. Wang, D. Rigueur and K. M. Lyons: TGFbeta signaling in cartilage development and maintenance. *Birth Defects Res C Embryo Today*, 102(1), 37-51 (2014) doi:10.1002/bdrc.21058
29. B. S. Yoon and K. M. Lyons: Multiple functions of BMPs in chondrogenesis. *J Cell Biochem*, 93(1), 93-103 (2004) doi:10.1002/jcb.20211
30. M. M. Caron, P. J. Emans, D. A. Surtel, A. Cremers, J. W. Voncken, T. J. Welting and L. W. van Rhijn: Activation of NF-kappaB/p65 Facilitates Early Chondrogenic Differentiation during Endochondral Ossification. *PloS one*, 7(3), e33467 (2012) doi:10.1371/journal.pone.0033467
31. F. Spaapen, G. G. van den Akker, M. M. Caron, P. Prickaerts, C. Rofel, V. E. Dahlmans, D. A. Surtel, Y. Paulis, F. Schweizer, T. J. Welting, L. M. Eijssen and J. W. Voncken: The immediate early gene product EGR1 and polycomb group proteins interact in epigenetic programming during chondrogenesis. *PLoS One*, 8(3), e58083 (2013) doi:10.1371/journal.pone.0058083
32. T. Atsumi, Y. Miwa, K. Kimata and Y. Ikawa: A chondrogenic cell line derived from a differentiating culture of AT805 teratocarcinoma cells. *Cell Differ Dev*, 30(2), 109-16 (1990)
33. T. J. Welting, M. M. Caron, P. J. Emans, M. P. Janssen, K. Sanen, M. M. Coolsen, L. Voss, D. A. Surtel, A. Cremers, J. W. Voncken and L. W. van Rhijn: Inhibition of cyclooxygenase-2 impacts chondrocyte hypertrophic differentiation during endochondral ossification. *Eur Cell Mater*, 22, 420-36; discussion 436-7 (2011)
34. M. D. Robinson, D. J. McCarthy and G. K. Smyth: edgeR: a Bioconductor package for differential expression analysis of digital gene expression data. *Bioinformatics*, 26(1), 139-40 (2010) doi:10.1093/bioinformatics/btp616
35. D. J. McCarthy, Y. Chen and G. K. Smyth: Differential expression analysis of multifactor RNA-Seq experiments with respect to biological variation. *Nucleic Acids Res*, 40(10), 4288-97 (2012) doi:10.1093/nar/gks042
36. E. Y. Chen, C. M. Tan, Y. Kou, Q. Duan, Z. Wang, G. V. Meirelles, N. R. Clark and A. Ma'ayan: Enrichr: interactive and collaborative HTML5 gene list enrichment analysis tool. *BMC Bioinformatics*, 14, 128 (2013) doi:10.1186/1471-2105-14-128
37. R. W. Farndale, C. A. Sayers and A. J. Barrett: A direct spectrophotometric microassay for sulfated glycosaminoglycans in cartilage cultures. *Connective tissue research*, 9(4), 247-8 (1982)
38. C. A. Goodman and T. A. Hornberger: Measuring protein synthesis with SUnSET: a valid alternative to traditional techniques? *Exerc Sport Sci Rev*, 41(2), 107-15 (2013) doi:10.1097/JES.0b013e3182798a95
39. C. J. Henrich: A Microplate-Based Nonradioactive Protein Synthesis Assay: Application to TRAIL Sensitization by Protein Synthesis Inhibitors. *PLoS One*, 11(10), e0165192 (2016) doi:10.1371/journal.pone.0165192
40. T. A. McCaffrey, L. A. Agarwal and B. B. Weksler: A rapid fluorometric DNA assay for the measurement of cell density and proliferation in vitro. *In Vitro Cell Dev Biol*, 24(3), 247-52 (1988) doi:10.1007/bf02623555
41. A. C. Panda, J. L. Martindale and M. Gorospe: Polysome Fractionation to Analyze mRNA Distribution Profiles. *Bio-protocol*, 7(3), e2126 (2017) doi:10.21769/BioProtoc.2126
42. N. Deniz, E. M. Lenarcic, D. M. Landry and S. R. Thompson: Translation initiation factors are not required for Dicistroviridae IRES function in vivo. *Rna*, 15(5), 932-46 (2009) doi:10.1261/rna.1315109
43. A. J. Collier, S. Tang and R. M. Elliott: Translation efficiencies of the 5' untranslated region from representatives of the six major genotypes of hepatitis C virus using a novel bicistronic reporter assay system. *J Gen Virol*, 79 (Pt 10), 2359-66 (1998) doi:10.1099/0022-1317-79-10-2359
44. P. S. Ray, R. Grover and S. Das: Two internal ribosome entry sites mediate the translation of p53 isoforms. *EMBO Rep*, 7(4), 404-10 (2006) doi:10.1038/sj.embor.7400623
45. V. Lefebvre, M. Angelozzi and A. Haseeb: SOX9 in cartilage development and disease. *Curr Opin Cell Biol*, 61, 39-47 (2019) doi:10.1016/j.ceb.2019.07.008
46. C. F. Liu, M. Angelozzi, A. Haseeb and V. Lefebvre: SOX9 is dispensable for the initiation of

epigenetic remodeling and the activation of marker genes at the onset of chondrogenesis. *Development*, 145(14) (2018) doi:10.1242/dev.164459
47. M. M. Caron, P. J. Emans, D. A. Surtel, P. M. van der Kraan, L. W. van Rhijn and T. J. Welting: BAPX-1/NKX-3.2 acts as a chondrocyte hypertrophy molecular switch in osteoarthritis. *Arthritis Rheumatol*, 67(11), 2944-56 (2015) doi:10.1002/art.39293
48. S. Yamashita, M. Andoh, H. Ueno-Kudoh, T. Sato, S. Miyaki and H. Asahara: Sox9 directly promotes Bapx1 gene expression to repress Runx2 in chondrocytes. *Exp Cell Res*, 315(13), 2231-40 (2009) doi:10.1016/j.yexcr.2009.03.008
49. C. F. Liu and V. Lefebvre: The transcription factors SOX9 and SOX5/SOX6 cooperate genome-wide through super-enhancers to drive chondrogenesis. *Nucleic Acids Res*, 43(17), 8183-203 (2015) doi:10.1093/nar/gkv688
50. P. A. Trainor and A. E. Merrill: Ribosome biogenesis in skeletal development and the pathogenesis of skeletal disorders. *Biochim Biophys Acta*, 1842(6), 769-78 (2014) doi:10.1016/j.bbadis.2013.11.010
51. G. Venturi and L. Montanaro: How Altered Ribosome Production Can Cause or Contribute to Human Disease: The Spectrum of Ribosomopathies. *Cells*, 9(10) (2020) doi:10.3390/cells9102300
52. R. J. Dowling, I. Topisirovic, T. Alain, M. Bidinosti, B. D. Fonseca, E. Petroulakis, X. Wang, O. Larsson, A. Selvaraj, Y. Liu, S. C. Kozma, G. Thomas and N. Sonenberg: mTORC1-mediated cell proliferation, but not cell growth, controlled by the 4E-BPs. *Science*, 328(5982), 1172-6 (2010) doi:10.1126/science.1187532
53. E. Jan and P. Sarnow: Factorless ribosome assembly on the internal ribosome entry site of cricket paralysis virus. *J Mol Biol*, 324(5), 889-902 (2002) doi:10.1016/s0022-2836(02)01099-9
54. A. C. Godet, F. David, F. Hantelys, F. Tatin, E. Lacazette, B. Garmy-Susini and A. C. Prats: IRES Trans-Acting Factors, Key Actors of the Stress Response. *Int J Mol Sci*, 20(4) (2019) doi:10.3390/ijms20040924
55. N. Chaichanit, M. Wonglapsuwan and W. Chotigeat: Ribosomal protein L10A and signaling pathway. *Gene*, 674, 170-177 (2018) doi:10.1016/j.gene.2018.06.081
56. Z. Shi, K. Fujii, K. M. Kovary, N. R. Genuth, H. L. Röst, M. N. Teruel and M. Barna: Heterogeneous Ribosomes Preferentially Translate Distinct Subpools of mRNAs Genome-wide. *Mol Cell*, 67(1), 71-83.e7 (2017) doi:10.1016/j.molcel.2017.05.021
57. D. Tong, J. Zhang, X. Wang, Q. Li, L. Y. Liu, J. Yang, B. Guo, L. Ni, L. Zhao and C. Huang: MeCP2 facilitates breast cancer growth via promoting ubiquitination-mediated P53 degradation by inhibiting RPL5/RPL11 transcription. *Oncogenesis*, 9(5), 56 (2020) doi:10.1038/s41389-020-0239-7
58. Q. Hao, J. Wang, Y. Chen, S. Wang, M. Cao, H. Lu and X. Zhou: Dual regulation of p53 by the ribosome maturation factor SBDS. *Cell Death Dis*, 11(3), 197 (2020) doi:10.1038/s41419-020-2393-4
59. S. Xue, S. Tian, K. Fujii, W. Kladwang, R. Das and M. Barna: RNA regulons in Hox 5' UTRs confer ribosome specificity to gene regulation. *Nature*, 517(7532), 33-38 (2015) doi:10.1038/nature14010
60. K. Noben-Trauth and J. R. Latoche: Ectopic mineralization in the middle ear and chronic otitis media with effusion caused by RPL38 deficiency in the Tail-short (Ts) mouse. *The Journal of biological chemistry*, 286(4), 3079-3093 (2011) doi:10.1074/jbc.M110.184598
61. G. R. Mortier, D. H. Cohn, V. Cormier-Daire, C. Hall, D. Krakow, S. Mundlos, G. Nishimura, S. Robertson, L. Sangiorgi, R. Savarirayan, D. Sillence, A. Superti-Furga, S. Unger and M. L. Warman: Nosology and classification of genetic skeletal disorders: 2019 revision. *Am J Med Genet A*, 179(12), 2393-2419 (2019) doi:10.1002/ajmg.a.61366
62. H. Nakhoul, J. Ke, X. Zhou, W. Liao, S. X. Zeng and H. Lu: Ribosomopathies: mechanisms of disease. *Clin Med Insights Blood Disord*, 7, 7-16 (2014) doi:10.4137/CMBD.S16952
63. H. Heberle, G. V. Meirelles, F. R. da Silva, G. P. Telles and R. Minghim: InteractiVenn: a web-based tool for the analysis of sets through Venn diagrams. *BMC Bioinformatics*, 16, 169 (2015) doi:10.1186/s12859-015-0611-3
64. D. N. Slenter, M. Kutmon, K. Hanspers, A. Riutta, J. Windsor, N. Nunes, J. Melius, E. Cirillo, S. L. Coort, D. Digles, F. Ehrhart, P. Giesbertz, M. Kalafati, M. Martens, R. Miller, K. Nishida, L. Rieswijk, A. Waagmeester, L. M. T. Eijssen, C. T. Evelo, A. R. Pico and E. L. Willighagen: WikiPathways: a multifaceted pathway database bridging metabolomics to other omics research. *Nucleic Acids Res*, 46(D1), D661-D667 (2018) doi:10.1093/nar/gkx1064
65. M. Kutmon, M. P. van Iersel, A. Bohler, T. Kelder, N. Nunes, A. R. Pico and C. T. Evelo: PathVisio 3: an extendable pathway analysis toolbox. *PLoS Comput Biol*, 11(2), e1004085 (2015) doi:10.1371/journal.pcbi.1004085

Figure legends

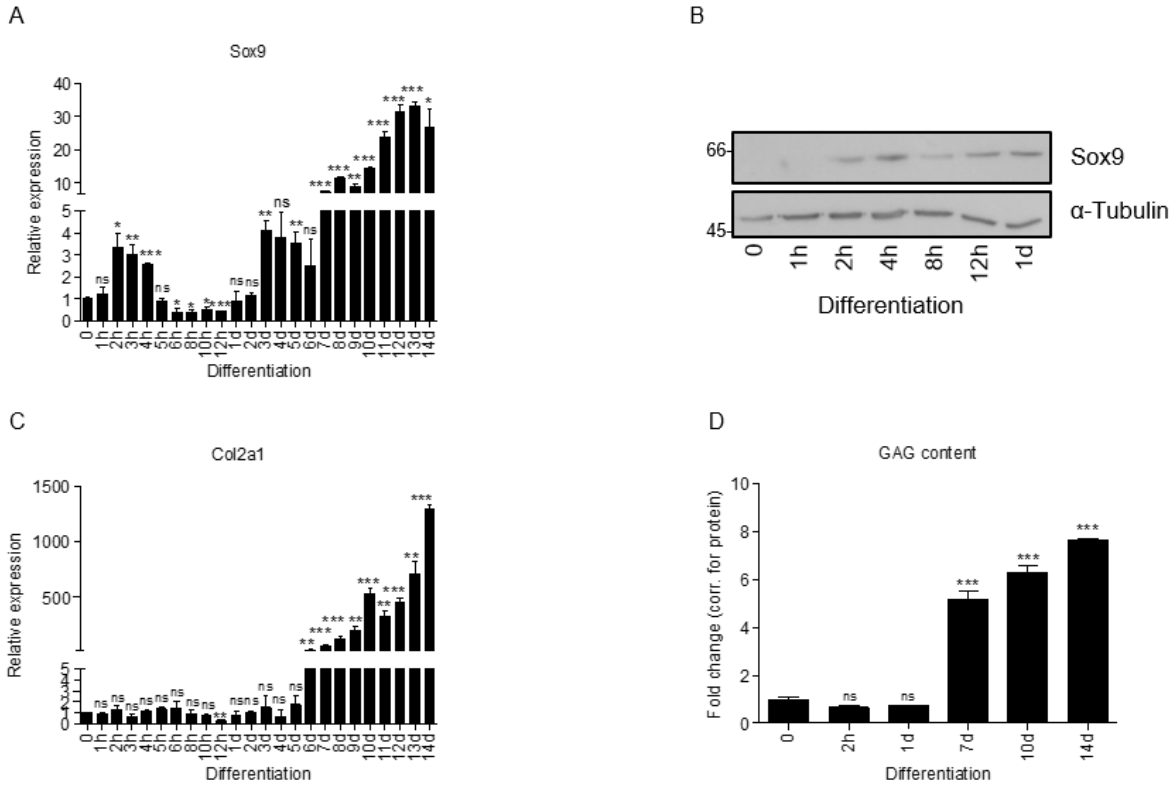

Figure 1: Sox9 expression has a bi-phasic peak expression during chondrogenic differentiation of ATDC5 cells

A: Sox9 mRNA expression showed bi-phasic peak pattern during ATDC5 differentiation (h=hours, d=days) as measured by RT-qPCR (30, 31). Results were normalized to β-Actin mRNA expression and presented relative to t=0. **B**: Sox9 protein expression peak during early ATDC5 differentiation as measured by immunoblotting. α-Tubulin was used as loading control. Molecular weight markers (in kDa) are shown on the left. **C**: In similar samples from (A), Col2a1 mRNA expression was measured during ATDC5 differentiation by RT-qPCR and showed an increase in expression from day 6 onwards. **D**: GAG content (by Alcian Blue staining and corrected for total protein expression) was determined during ATDC5 differentiation. Experiments were performed in triplicates, bars represent mean±SEM. ns= not significant, *=p<0.05, **=p<0.01, p=<0.0001.

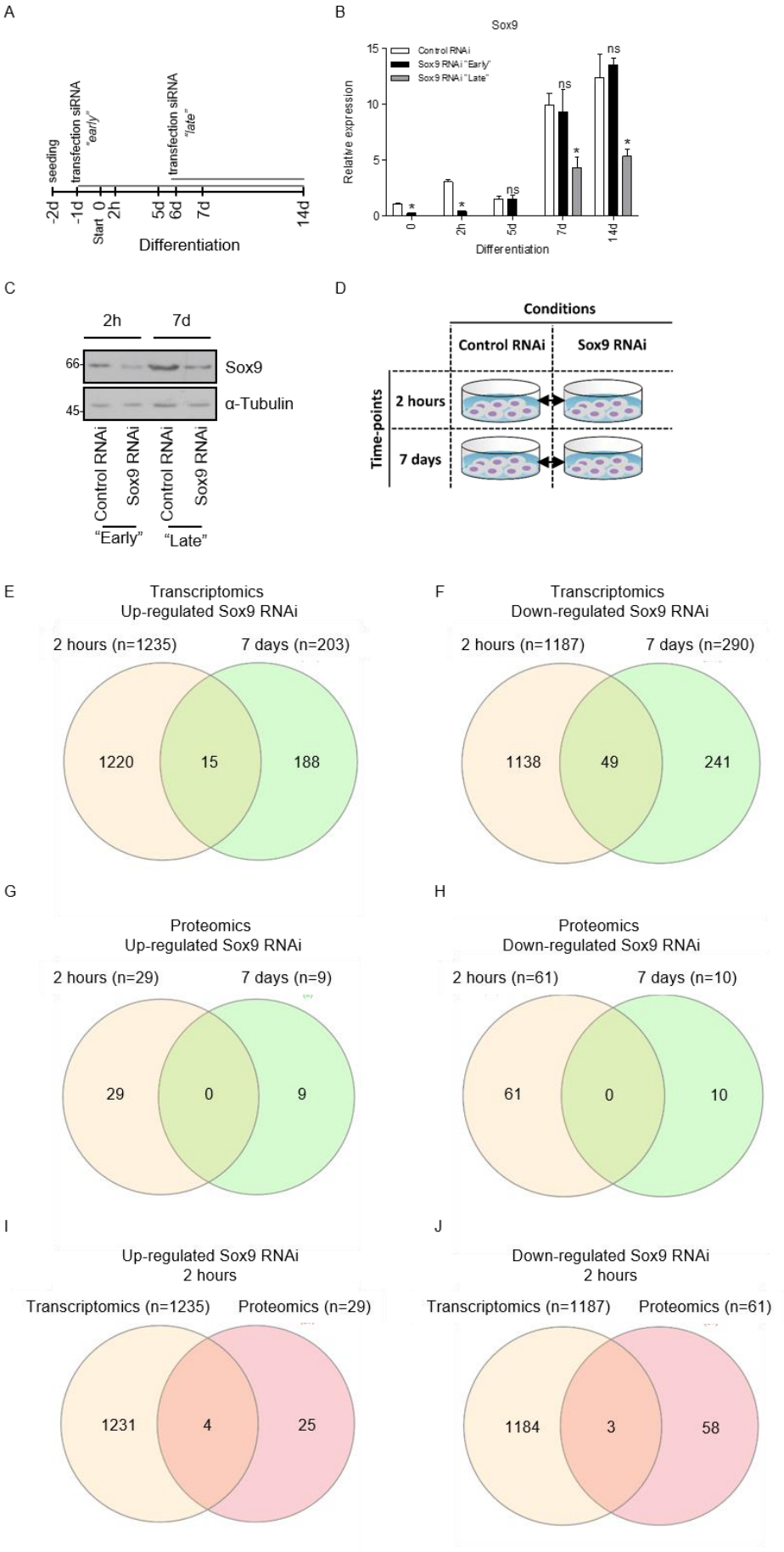
A
seeding
transfection siRNA "early"
transfection siRNA "late"
-2d
-1d
0
2h
5d
6d
7d
14d
Start
Differentiation
B
Sox9
Control RNAi
Sox9 RNAi "Early"
Sox9 RNAi "Late"
Relative expression
ns
*
0
2h
5d
7d
14d
Differentiation
C
2h
7d
66-
45-
Sox9
α-Tubulin
Control RNAi
Sox9 RNAi
Control RNAi
Sox9 RNAi
"Early"
"Late"
D
Conditions
Control RNAi
Sox9 RNAi
Time-points
2 hours
7 days
E
Transcriptomics
Up-regulated Sox9 RNAi
2 hours (n=1235)
7 days (n=203)
1220
15
188
F
Transcriptomics
Down-regulated Sox9 RNAi
2 hours (n=1187)
7 days (n=290)
1138
49
241
G
Proteomics
Up-regulated Sox9 RNAi
2 hours (n=29)
7 days (n=9)
29
0
9
H
Proteomics
Down-regulated Sox9 RNAi
2 hours (n=61)
7 days (n=10)
61
0
10
I
Up-regulated Sox9 RNAi
2 hours
Transcriptomics (n=1235)
Proteomics (n=29)
1231
4
25
J
Down-regulated Sox9 RNAi
2 hours
Transcriptomics (n=1187)
Proteomics (n=61)
1184
3
58

Figure 2: Elucidating the function of early Sox9 expression by transcriptome and proteome analyses

A: Schematic representation of experimental set-up for Sox9 knockdown experiment. Specific Sox9 RNAi (100 nM) or scrambled control RNAi (100 nM) were transiently transfected "early" at t=-1d or "late" t=6d. ATDC5 cells were differentiated from day 0 onwards and harvested for transcriptome and proteome analysis at at t=0, 2h, 5d, 7d, 14d. **B**: Sox9 mRNA expression during ATDC5 differentiation in Control and Sox9 RNAi conditions (h=hours, d=days) as measured by RT-qPCR. Results were normalized to β-Actin RNA expression and presented relative to t=0. Bars represent mean±SEM. ns= not significant, *=p<0.05, **=p<0.01, p=<0.0001. **C**: Sox9 protein expression at t=2h (for "early knockdown condition) and t=7d (for "late" knockdown conditions) time point in Control and Sox9 RNAi conditions as measured by immunoblotting. α-Tubulin was used as loading control. Molecular weight markers (in kd) are shown on the left. **D**: Schematic representation of time points and comparisons for transcriptomics and proteomics analysis. **E**: Venn diagram (63) showing the numbers of genes whose expression was significantly upregulated upon Sox9 knockdown at 2 hours versus 7 day condition. **F**: Venn diagram showing the numbers of genes whose expression was significantly downregulated upon Sox9 knockdown at 2 hours versus 7 day condition. **G**: Venn diagram showing the numbers of proteins whose expression was significantly upregulated upon Sox9 knockdown at 2 hours versus 7 day condition. **H**: Venn diagram showing the numbers of proteins whose expression was significantly downregulated upon Sox9 knockdown at 2 hours versus 7 day condition. **I**: Venn diagram showing the upregulated genes versus proteins at 2 hours in differentiation. **J**: Venn diagram showing the downregulated genes versus proteins at 2 hours in differentiation.

Top 3 identified enriched pathways (Based on combined score)					
2 Hours					
RNA	*Pathway ID*	*Pathway description*	*P-value (p)*	*Adjusted p-value (q)*	*Combined score*
WikiPathway 2019	WP163	Cytoplasmic Ribosomal Proteins	3,67E-11	6,46E-09	77,64
(Mouse)	WP1248	Oxidative phosphorylation	3,86E-07	2,26E-05	45,24
	WP295	Electron Transport Chain	2,74E-07	2,41E-05	38,77
	Name		*P-value (p)*	*Adjusted p-value (q)*	*Combined score*
KEGG 2019	Ribosome		1,12E-10	3,39E-08	57,88
(Mouse)	Huntington disease		1,25E-08	1,90E-06	40,69
	Thermogenesis		3,69E-08	3,72E-06	35,49
Protein	*Pathway ID*	*Pathway description*	*P-value (p)*	*Adjusted p-value (q)*	*Combined score*
WikiPathway 2019	WP163	Cytoplasmic Ribosomal Proteins	5,96E-05	1,05E-02	117,49
(Mouse)	WP175	Acetylcholine Synthesis	3,11E-02	7,82E-01	110,19
	WP298	G13 Signaling Pathway	1,33E-02	5,86E-01	49,21
	Name		*P-value (p)*	*Adjusted p-value (q)*	*Combined score*
KEGG 2019	Glycolysis / Gluconeogenesis		3,43E-03	5,20E-01	56,47
(Mouse)	Pyruvate metabolism		1,27E-02	3,49E-01	51,09
	Ribosome		1,03E-03	3,11E-01	44,98

Figure 3: Early Sox9 expression is involved in ribosomal pathways

Top 3 identified enriched pathways from WikiPathway 2019 and KEGG2019 pathway analysis in control RNAi compared to Sox9 RNAi at 2 hours condition in ATDC5 differentiation for transcriptome and proteome data sets.

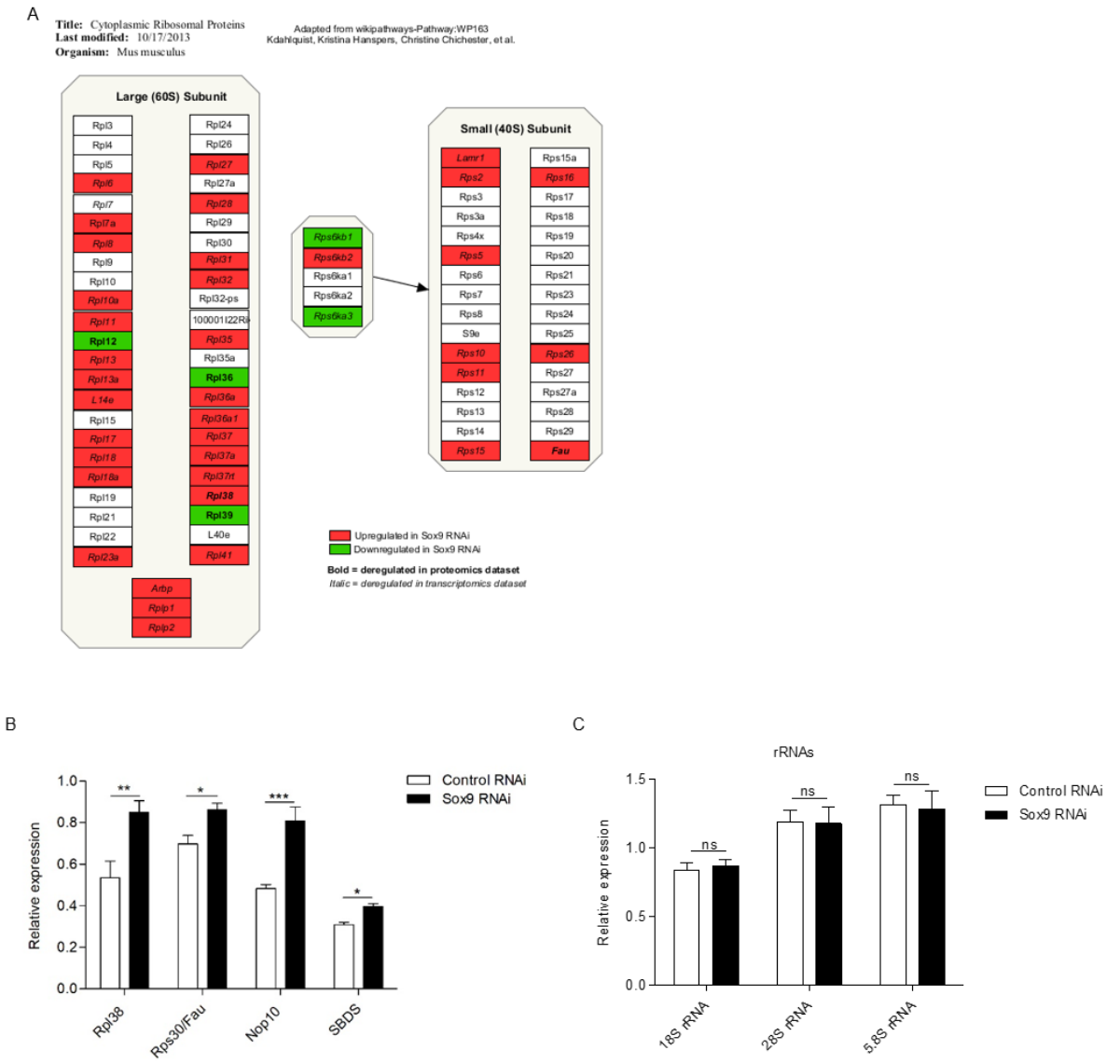

Figure 4: Early Sox9 regulates ribosomal protein expression

A: Schematic representation of significantly differentially expressed ribosomal proteins from transcriptome and proteome datasets based on Wikipathways (64): WP163 using PathVisio 3 (65). **B**: Rpl38, Rps30/Fau, Nop10 and SBDS expression at 2 hours in ATDC5 differentiation in Control and Sox9 RNAi conditions as measured by RT-qPCR. Results were normalized to β-Actin RNA expression and presented relative to t=0. **C**: In similar samples from B; 18S rRNA, 28S rRNA and 5.8S rRNA expression. Bars represent mean±SEM. ns= not significant, *=p<0.05, **=p<0.01, p=<0.0001.

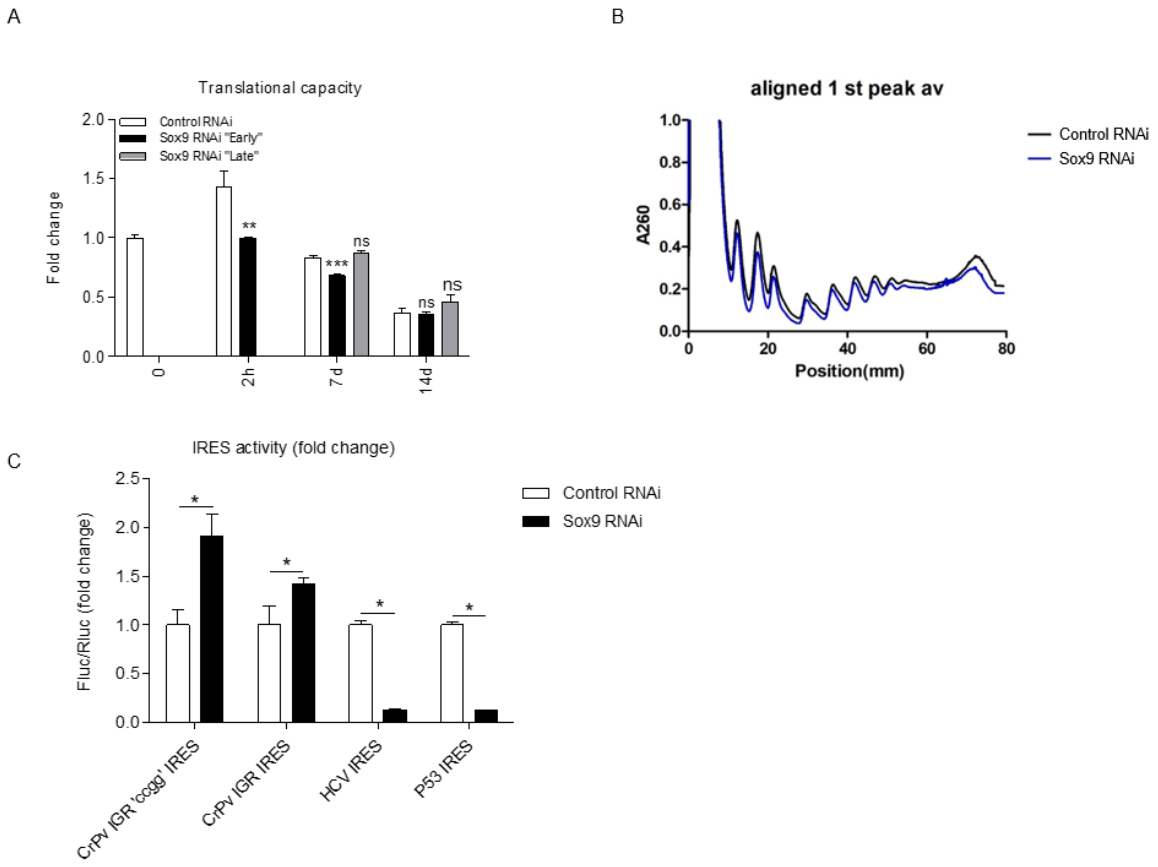

Figure 5: Knockdown of early Sox9 expression leads to a reduced translational capacity, lower amount of ribosomes and alters ribosome modus

A: Total protein translation measurements based on puromycin incorporation was normalized to total DNA content per well (Mean±SEM, n=6/group) at indicated time points. **B**: Polysome fractionation of control and Sox9 knock-down cells (Mean only, n=3/group) after 2 hours of differentiation. **C**: Ribosome modus was assessed for the CrPv IGR CCGG mutant IRES, the intact CrPv IGR IRES, the HCV IRES and the P53 IRES after 24 hours of differentiation. Bars represent mean±SEM. ns= not significant, *=p<0.05, **=p<0.01, p=<0.0001.

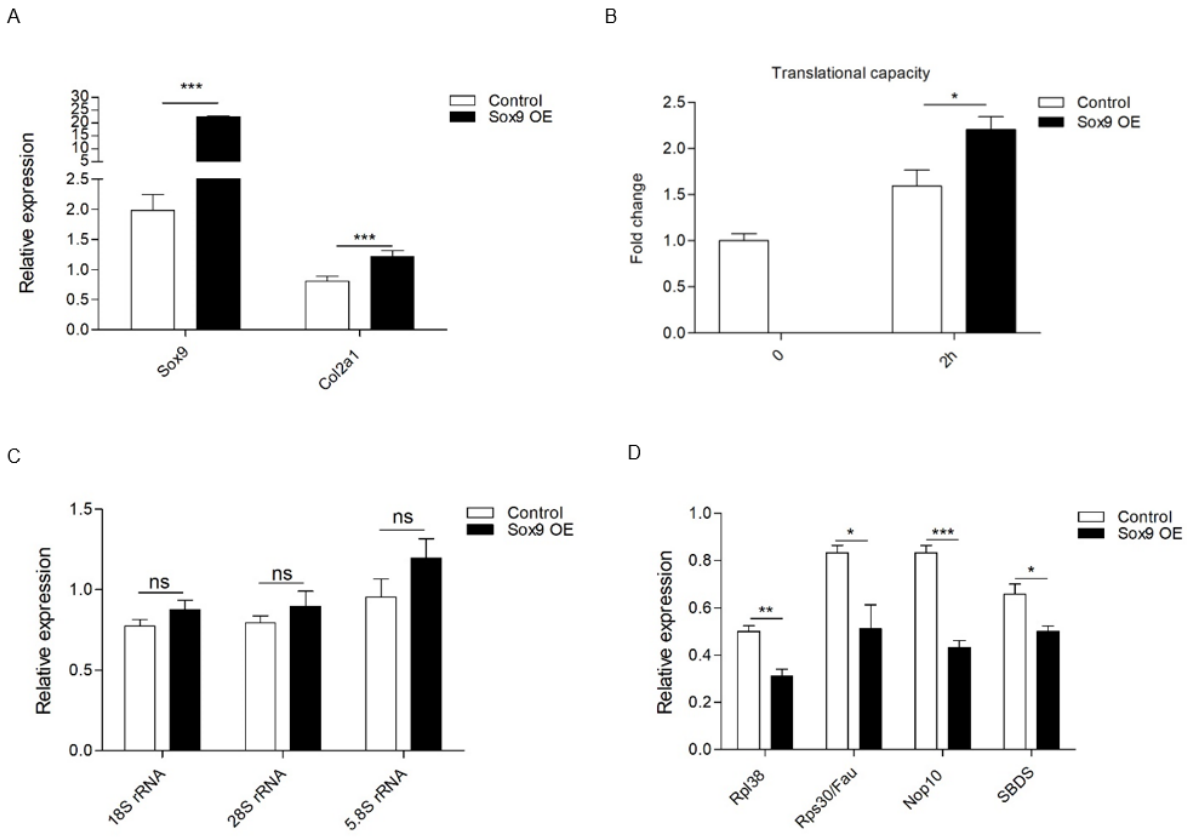

Figure 6: Overexpression of early Sox9 leads to an increased translational capacity

A: Sox9 mRNA expression at 2 hours in ATDC5 differentiation in Control and Sox9 overexpression (OE) conditions as measured by RT-qPCR. Results were normalized to β-Actin RNA expression and presented relative to t=0. **B:** Total protein translation measurements based on puromycin incorporation was normalized to total DNA content per well (Mean±SEM, n=6/group) at indicated time points. **C**: In similar samples from A; 18S rRNA, 28S rRNA and 5.8S rRNA expression at 2 hours in ATDC5 differentiation in Control and Sox9 overexpression conditions. **D:** In similar samples from A; Rpl38, Rps30/Fau, Nop10 and SBDS expression at 2 hours in ATDC5 differentiation in Control and Sox9 overexpression conditions. Bars represent mean±SEM. ns= not significant, *=p<0.05, **=p<0.01, p=<0.0001.